XIV International Conference on Building Pathology and Constructions Repair – CINPAR 2018

Numerical study on the reduction of the seismic vulnerability of historical industrial buildings with wide timber roofs

Natalino Gattesco[a], Ingrid Boem[b*]

[a]*University of Trieste, piazzale Europa 1, Trieste 34127, Italy*
[b]*University of Trieste, piazzale Europa 1, Trieste 34127, Italy*

Abstract

In the paper are presented the results of a preliminary numerical study concerning the evaluation of the effectiveness of interventions for the reduction of the seismic vulnerability of buildings with traditional multiple sloping timber roofs laid on masonry walls along the building perimeter and on columns internally. In particular, the effects of three different strengthening strategies are analyzed: the bracing of the roof diaphragm by means of wooden-based nailed panels, the addition of steel portal frames and the reinforcement of the masonry through the application of a mortar coating with composite meshes embedded. To take into account the different interventions effects, a simplified numerical procedure, based on non-linear-static analysis, is proposed and a case study is analyzed numerically to compare, in terms of resistant ground acceleration, $a_{g,res}$, the effects of the different reinforcement techniques. Typically, the absence of the roof diaphragm determines the out-of-plane collapse of the longitudinal walls, for very low seismic actions. The roof stiffening induces a redistribution of the seismic load from the longitudinal walls to the transversal ones; however, as they are not dimensioned for horizontal loads, very modest benefits emerged in terms of $a_{g,res}$. The addition of two steel portal frames or the reinforcement of the walls with the reinforced mortar technique permits to reach values of the resistant acceleration considerably higher than that of the unreinforced configuration (1.91 and 2.73 times higher, respectively).

Keywords: Type your keywords here, separated by semicolons ;

* Corresponding author. Tel.: +39-040-5583840.
  E-mail address: boem@dicar.units.it

1. Introduction

Typically, historical industrial buildings present traditional multi-sloping timber roofs laid on masonry walls along the building perimeter and on point supports internally, such as wooden studs, steel columns or masonry pillars. Many of these structures are part of the architectural heritage and constitute important testimonies of the historical and cultural identity of the territory in which they rise. Therefore, it is the need to maintain these assets, ensuring their safe usability and the preservation of the structures and their contents. Thus, it is necessary to identify effective and compatible strategies to overcome the structural deficiencies that these types of buildings have against the seismic action, behaving as a series of independent frames which are not able to effectively distribute the seismic loads among the transversal walls.

The paper provides indications on the characteristics and the performances of the main strategies to adopt for strengthening these structures, giving also the methods to quantify their contribution. The considered methods concern the bracing of the roof by means of wooden based nailed panels, the introduction of steel portal frames and the reinforcement of the perimeter walls by means of a mortar coating with composite meshes embedded.

A case study, representing a typical configuration, is illustrated, with an assessment of the seismic performances before and after the reinforcement measures. The modeling strategy is described in detail, indicating simplified methods to take into account the different interventions; their effectiveness is then evaluated by means of non-linear static analysis.

2. Strengthening strategies

2.1. Bracing of the timber roof

The technique consists in the application of wooden based or CLT (Cross Laminated Timber) adjacent panels above the main joists of the roof and connected by nails or screws along the perimeter. It is observed that, in order to guarantee an adequate stiffness, the panels have to be nailed on their whole perimeter and thus it could be necessary to introduce some additional wooden elements to the main timber frame of the roof or, as an alternative, to use metal strips connecting adjacent panels. The analytical procedure to evaluate the stiffness and the resistance capacity of these bracing elements has already been analyzed in detail by the authors for timber walls with nailed sheathing (Gattesco and Boem, 2016) and is here summarized.

Considering a roof portion between two adjacent principal rafters, the elastic stiffness of the bracing system composed of n nailed panels, K_{tot}, can be evaluated analytically considering the contributions to deformability of the n panels of the segment, δ_i:

$$K_{tot} = \frac{1}{H^2} \sum_{i=1}^{n} \frac{h_i^2}{\delta_i} = \frac{1}{H^2} \sum_{i=1}^{n} \frac{h_i^2}{\delta_{s,i} + \delta_{ns,i}},$$ (1)

where H is the rafter length and h_i the panel height. $\delta_{s,i}$ represents the displacement due to shear deformation in the sheathing panel and $\delta_{ns,i}$ represents the displacements due to the slip in the nailed connections between the sheathing and the timber frame:

$$\delta_{s,i} = \frac{h_i}{Gb_i t}, \qquad \delta_{ns,i} = \delta_{nsx,i} + \delta_{nsy,i} = \frac{p}{K_{pf} b_i} 2(1 + \frac{h_i}{b_i}),$$ (2)

being b_i panel width, t the thickness and G its shear modulus; p is the nail spacing and K_{pf} the slip modulus per shear plane of the single nailed connection, which can be evaluated experimentally or calculated according with the method indicated in Eurocode 5, as function of panel density (ρ_m) and fastener diameter (d):

$$K_{pf} = \frac{\rho_m^{1.5} d^{0.8}}{30}, \text{ without hole predrilling.}$$ (3)

For the calculation of the load-bearing capacity of a bracing segment, $F_{v,i}$, the simplified model proposed in Eurocode 5, based on the hypothesis of a pure shear stress acting along the perimeter of the panel, can be adopted. It is assumed that each nail is stressed in the direction of the timber element to which it is connected for a force equal to

its plastic resistance, f_{nail}, which can be evaluated experimentally or calculated analytically (e.g. as Eurocode 5 relationships).

For a correct estimation of the load bearing capacity of a roof segment by applying this simplified method, it is necessary to consider a nail resistance (and stiffness - Gattesco and Boem, 2015a) increased by 20%. The global capacity of the segmented panel F_v, can be calculated as the sum of the resistances $F_{v,i}$ of the n segments:

$$F_v = \sum_{i=1}^{n} F_{v,i} \text{ , with } F_{v,i} = \frac{1.2 \cdot f_{nail} \cdot b_i \cdot c_i}{p} \text{ (} c_i = 1 \text{ with } b_i > h_i/2, \, c_i = 2b_i/h_i \text{ otherwise).} \tag{4}$$

The stiffness k_i and the resistance $F_{v,i}$ of a segment with an opening can prudentially be neglected.

The ultimate displacement of the bracing can be assumed equal to 0.7% of the rafter length. This value is derived from experimental cyclic tests carried out on timber walls, excluding the contribution due to the deformability of the base connections. It is, however, necessary to evaluate the compatibility of the horizontal displacements of the roof with the out-of-plane deflection of the perimeter walls.

It is observed that effective connections of the braced roof with the perimeter walls are essential to ensure the diaphragm action, so that the roof is able to constrain the out-of-plane deformation of the walls and transfer the horizontal seismic loads to the seismic-resistant elements, in the earthquake direction. Therefore, it is necessary to complete the roof main frame with timber elements which have to be effectively connected at the top of the perimeter walls (e.g. Sisti et al., 2016).

2.2. Steel portal frames

The intervention, suitable for multiple-aisle buildings, consists in inserting one or more metallic portal frames in the one or both directions, so to stiffen the structure, contain the deflection of the perimeter walls and increase the resistance in the horizontal direction. The portal frames are generally composed of steel profiles (usually UPN pairs or HE) jointed with bolted joints and steel plates. The timber roof has to be effectively connected to the portal frames by means of steel hangers. Moreover, the posts of the portal frame has to be connected to the perimeter wall by means of injected bars. An adequate foundation system, able to contrast uplifts induced by the seismic actions (e.g. ballast or micropiles), is also of fundamental importance. The static scheme generally considered for portal frames is that of a reticular portal frame (pinned nodes).

2.3. Reinforced mortar coating

The technique consists in the application, on both sides of the wall, of a layer of mortar (approximately 30 mm thick) with an embedded reinforcement made of composite meshes based, for example, on glass (GFRP) or carbon (CFRP) fibers (Fig. 1). The effectiveness of this modern technique for improving the masonry performances in respect of both in plane and out-of-plane actions has been evaluated through broad experimental investigations, numerical studies and analytical evaluations (Gattesco and Boem, 2015b; Gattesco and Boem, 2017a).
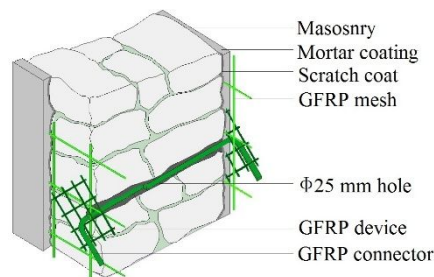

Fig. 1. Schematization of considered reinforced mortar coating technique

A schematization of the behavior of a reinforced wall subjected to out-of-plane action is illustrate in Fig. 2a. According to Gattesco and Boem, 2017b, the first cracking moment of a reinforced masonry section can be evaluated neglecting the mesh contribution and applying the superposition principle:

$$M_{cr(R)} = \left(\frac{N}{A_{id}} + \frac{|f_{f,c}|}{\alpha_c} \right) W_{id} ,$$ (5)

with A_{id} e W_{id} cross section area and the resistance modulus of the uncracked section idealized to masonry, $f_{f,c}$ flexural tensile strength of mortar coating and α_c modular ratio between the coating and the masonry (E_c/E_m).

The maximum bending moment can be calculated considering a cracked section composed by only compressed mortar and by the tensed GFRP wires:

$$M_{u(R)}(N) = 0.8x \cdot f_{c,c} \cdot b \left(\frac{h_{TOT}}{2} - 0.4x \right) + n_w T_w \left(\frac{h_{TOT}}{2} - c \right) \quad \text{con} \quad x = \frac{N + n_w T_w}{0.8 \, f_{c,c} \cdot b} ,$$ (6)

being n_w the number of GFRP tensed wires in the cross section, T_w the tensile resistance of one wire, x the neutral axis depth, $f_{c,c}$ the compressive strength of the mortar of the coating, h_{TOT} and b the global depth and the width of the cross section and c the wires cover.

The elastic stiffness of the reinforced wall, $K_{(R)}$, can be calculated considering the flexural deformability of the element. The last displacement, $s_{u,(R)}$, can be evaluated, approximately, omitting the contribution of the elastic deformation (which is negligible for the reinforced plaster), considering the plastic curvature at the base, ϕ_p, and the "plasticized length" (cracked masonry), l_p, when the ultimate bending moment at the base is reached:

$$s_{u(R)} = l \cdot \frac{l_P \phi_P}{2} = \frac{l^2}{2} \left(1 - \frac{M_{cr(R)}}{M_{u(R)}} \right) \cdot \frac{\varepsilon_{u,w}(1-\eta)}{h_{TOT} - c} ,$$ (7)

with l height of the wall, $\varepsilon_{u,w}$ ultimate mesh strain and $(1-\eta)$ part of the distance among cracks over which slip between wire and mortar occurs (may be assumed equal to 0.8 according to some tension tests carried out on reinforced mortar coating samples – Gattesco and Boem, 2017b).

The premature collapse of the wall in shear can be prudentially estimated considering the compressive action N ($V_{Rd} = \mu N$, with μ coefficient of static friction, typically 0.4 for masonry). Moreover, to ensure the reinforcement effectiveness, it is also necessary to respect the minimum anchorage and overlap lengths and to design adequate connections with the foundation.

A schematization of the shear behavior of a reinforced wall subjected to in-plane action is illustrate in Fig. 2b. According to Gattesco and Boem, 2017c, the resistance associated to the diagonal cracking mechanism can be assessed by applying the Turnsek-Cacovic (1971) formulation:

$$V_{(R)P} = b_P \cdot t \cdot \frac{1.5 \, f_{v,0(R)}}{\alpha} \sqrt{1 + \frac{\sigma}{1.5 \, f_{v,0(R)}}} \quad \text{with} \quad \alpha = \begin{cases} 1.5 & 1.5 \le l_P/b_P \\ l_P/b_P & 1 \le l_P/b_P \le 1.5 \\ 1.0 & l_P/b_P \le 1.0 \end{cases} ,$$ (8)

with b_p, l_p and t width, height and thickness of the masonry and σ the vertical compressive stress. The shear strength of the reinforced masonry, $f_{v,0(R)}$, can be evaluated by adopting the analytical approach proposed in Gattesco and Boem, (2015b), considering the shear strength of the unreinforced masonry, $f_{v,0(U)}$, and the tensile resistance of the mortar of the coating, $f_{t,c}$:

$$f_{v,0(R)} = \beta \left(f_{v,0(U)} + \frac{t_c}{t} f_{t,c} \right) ,$$ (9)

β is a coefficient that takes into account the interaction between the masonry and the reinforced mortar coating.

For the bending behavior (Fig. 2c), an elastic-plastic behavior with hardening can be considered. The ultimate resistance, $M_{P(R)}$, can be calculated considering only the contribution in tension of the composite mesh wires, applying an approach similar to that adopted for Equation (6). The moment associated to yielding, $M_{0(R)}$, can be evaluated using equation (10):

$$M_{0(R)} = -N \left(x_I - x_{II} \right) \cdot \frac{1}{1 - \frac{EI_{II}}{EI_I}} ,$$ (10)

where N is the axial force, x_I, E_I and E_{II}, x_{II} are the depth of the neutral axis and the flexural stiffness in pure bending for uncracked (I) and cracked (II) states. The ultimate in-plane displacement can be prudentially evaluated assuming a ductility equal to 6.
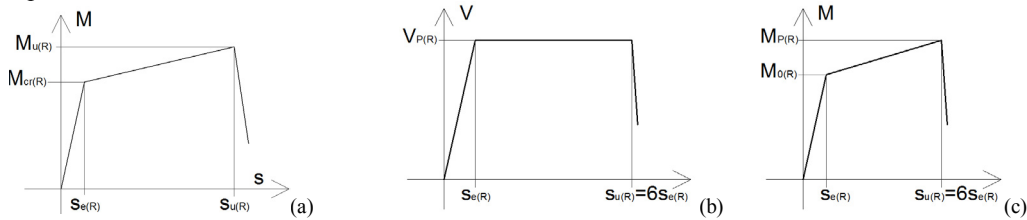

Fig. 2. Behavior of masonry walls strengthened with the reinforced mortar coating technique: (a) out-of-plane performances and in-plane performances due to (b) diagonal cracking and (c) bending mechanism

3. Method

In the simplified modeling proposed, based on nonlinear-static analysis, the main frame of the timber roof is schematized through beam elements. Non-structural and variable gravitational loads are taken into account by applying linear loads on these mono-dimensional elements. Pairs of equivalent springs, with non-linear axial behavior (elastic - perfectly plastic, with symmetrical behavior) are arranged along the diagonals between adjacent principal rafters (Fig. 3a).

The spring stiffness K_{eq}, resistance F_{eq}, and ultimate displacement $s_{u,eq}$ can be calculated, respectively, from the effective stiffness K_{tot}, resistance F_v and ultimate displacement $s_{u,tot}$, of the bracing, (see 2.1).

$$K_{eq} = K_{tot} \frac{H^2 + B^2}{2B^2}, \qquad F_{eq} = F_v \frac{\sqrt{H^2 + B^2}}{2B}, \qquad s_{u,eq} = s_{u,tot} \frac{B}{\sqrt{H^2 + B^2}}, \qquad (11)$$

where B and H are the width and length of the bracing (distance between adjacent principal rafters and rafter length).

The internal point support (studs, columns or pillars) are schematized by means of truss elements pinned at the base. The presence of the transversal walls (gable walls) can be modeled by introducing mono-dimensional vertical elements with elastic behavior, equipped with localized "plastic hinges" able to take into account the in-plane nonlinearity of the wall to both in shear and bending (Fig. 2b-c). Similar, also the longitudinal walls, subject to out-of-plane action, can be schematized in the same way, introducing, in correspondence of each principal rafter, a mono-dimensional vertical element provided with localized plastic hinges (Fig. 2a).

The steel portal frames can modeled by means of pinned frames. A schematization of the numerical model is reported in Fig. 3b.
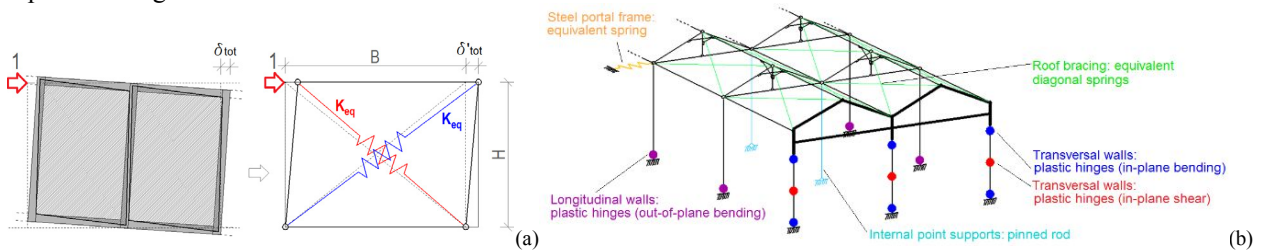

Fig. 3. Modeling of a roof bracing by means of equivalent diagonal non-linear axial springs (a) and schematization of the numerical model proposed for the evaluation of the seismic vulnerability of traditional masonry structures with multi-sloping timber roofs (b)

4. Case study

The analyzed case study concerns an ancient tram depot; the structure in a single level masonry building with a regular rectangular plan of dimensions 13400 x 64000 mm² (Fig. 4). The perimeter walls, 5700 mm high, are made of three-whyte solid brick masonry and have a thickness of 380 mm (self weight $\gamma = 18$ kN/m³, compressive strength $f_{c,m}$ = 3.2 MPa, Young modulus E_m = 1500 MPa, shear strength $f_{v,0}$ = 0.08 MPa). The sloping roof is composed of two

aisles, 6700 mm width, made of red spruce principal rafters arranged at a distance of 4000 m. A row of timber posts supports internally the roof. The roof is completed with parallel timber joists of reduced section supporting a layer of flat tiles and the bend tiles cover. The whole roof mass, referred to the seismic combination, was evaluated equal to 144 kg/m^2 (quasi permanent factor equal to zero for live loads).
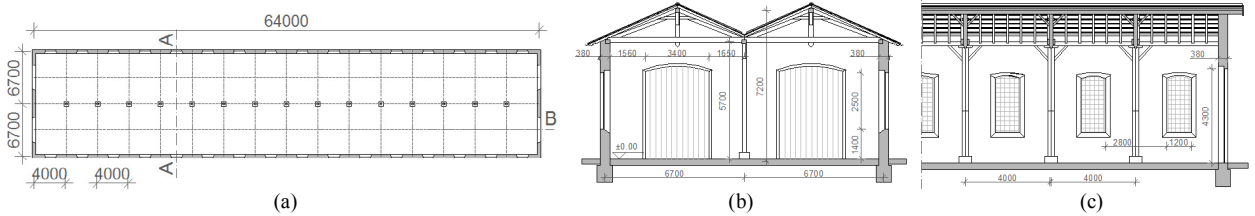

Fig. 4. Case study: (a) plan, (b) transversal section A-A and (c) longitudinal section B-B

Referring to the transversal direction, a first evaluation of the seismic vulnerability of the structure as built was carried out; then, the performances obtainable by applying the various proposed intervention solutions are analysed and compared.

It is observed that, in the actual situation (case "A"), due to the negligible diaphragm action of the roof, the collapse is governed by the out-of-plane overturning of the longitudinal walls. Referring to this mechanism, a non-linear kinematic analysis was carried out (according to CSLP, 2009), to determine the resistant ground acceleration a_g. The assessment of the seismic vulnerability was carried out considering a 4000 m-wide wall strip (distance between adjacent trusses - Fig. 5a): the capacity curve was calculated in function of the horizontal load multiplier α in the initial configuration (α_0) and of the displacement d_k of the control point corresponding to $\alpha = 0$ ($d_{k,0}$). The result provided a resisting ground acceleration $a_{g,res} = 0.121g$ (Fig. 5b).
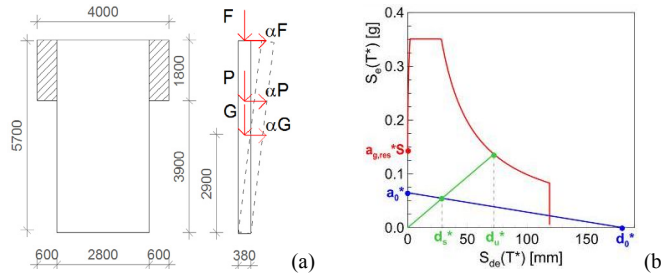

Fig. 5. Case "A": (a) configuration of the analysed wall portion, with indication of the considered kinematic mechanism and (b) evaluation of the resisting ground acceleration through non-linear kinematic analysis

When the strengthening interventions were considered, the assessment of seismic vulnerability was carried out according to the procedure indicated in CSLP, 2009, referring to the global capacity curve of the whole structure obtained by means of pushover analysis. A schematization of the numerical model is reported in Fig. 3.

The capacity curve of the reinforced building represents the value of the horizontal force in function of the displacement at the top of the transversal walls. It is observed that, in general, the results obtained by means of the global analysis of the structure are representative of its actual behavior when the mass activated by the first vibration mode is prevalent (indicatively, at least 80% of the whole mass). In a simplified way (FEMA 273), a diaphragm can be assumed rigid when its in-plane deflection, Δ_{rel}, evaluated on its length, L_S, does not exceed half of the ultimate displacement of the transversal walls cross-sections δ_u, evaluated on their height, H_T:

$$\frac{\Delta_{rel}}{L_S} \leq \frac{1}{2}\frac{\Delta_u}{H_T} \ . \tag{12}$$

For the analysed case study a first seismic vulnerability evaluation was performed on the structure with the reinforcement of the roof through nailed wooden-based panels (case "B"). In particular sheathing panels, 25 mm thick, 2000 mm wide and 3670 mm height were considered ($G = 1080$ MPa, $\rho_l = 650$ kg/m^3). The perimeter fasteners assumed are ϕ4/70 ring nails 50 mm spaced; its stiffness and strength characteristics were evaluated analytically, according to Section 2.1 ($K_{pf} = 1.62$ kN/mm and $f_{nail} = 1.89$ kN). The mass of the reinforced roof, referred to the

seismic combination, was evaluated equal to 160 kg/m^2. By applying the procedure described in Section 2.1, a stiffness K_{tot} equal to 12.88 kN/mm (K_{eq} = 11.86 kN/mm) and a resistance F_v equal to 181.52 kN (F_{eq} = 123.18 kN) were estimated for each bracing system. The ultimate equivalent displacement, $s_{u,eq}$, is equal to 18.9 mm. The performances of each transversal, unreinforced masonry wall were evaluated considering the resistant contribution of the three masonry piers (Fig. 4b), assuming a rigid spandrel, due to the dimensions of the gable. The resistance of these elements resulted governed by the bending failure mechanism (global wall resistance V_{Rd} = 184.0 kN). A halved masonry Young modulus was considered for the evaluation of the elastic stiffness, and a ductility equal to 4 was assumed for the evaluation of the ultimate displacement, according to the results of several experimental tests available in the literature (e.g. Magenes and Calvi, 1997).

From the numerical model it is observed that, when the transversal walls collapsed, the diagonal springs representing the roof bracing are still in the elastic range. In particular, the load in the springs reached 37.6 kN, close to transversal walls (Fig. 6a). The capacity curve of the structure (Fig. 7a) shows an initial linear-elastic trend up to about 3 mm, then the plasticization of the transversal walls starts, at a load of about 368 kN. At the reaching of the transversal walls ultimate displacement (10.6 mm), the roof deflection results equal to 16.3 mm. The global equivalent stiffness of the roof diaphragm in the horizontal plane is, therefore, 22.6 kN/mm, while the resistant ground acceleration $a_{g,res}$ is equal to 0.135g.

In order to increase the load-bearing capacity of the structure in the transversal direction, two steel portal frames were then introduced ("Case C"), which are able also to further limit the roof deflection. The portal frame configuration was made with HEA200, steel grade S275. The lateral stiffness of the portal was evaluated numerically, through linear-elastic analysis on a pinned frame model, and resulted equal to 21.2 kN/mm. The global capacity curve (Fig. 7a) showed an initial linear-elastic trend up to about 2.7 mm (291.5 kN/mm); then, as the plasticization of the transversal walls occurred, at 757.6 kN, a second linear phase, with reduced stiffness (26.3 kN/mm) was observed, until their collapse (at 974.5 kN). At the reaching of their ultimate displacement (10.6 mm), the maximum force in the roof equivalent diagonal springs was significantly lower than the resistance (58.8 kN - Fig. 6b) and was reasonably greater near the portal frames. At global ultimate displacement, the maximum horizontal displacement of the roof, with respect to the transverse walls, was 15.9 mm; the resistant acceleration was resulted equal to $a_{g,res}$ = 0.231 g.

As an alternative to portal frames, the strengthening of the perimeter walls by applying a reinforced mortar coating ("Case D") can be an effective solution. In particular, for the case study, a mixed cement-lime mortar coating (average compressive strength 7 MPa, tensile strength 1 MPa, Young modulus of 14.5 GPa), 30 mm thick, with GFRP meshes embedded (grid pitch 66x66 mm^2, single-wire tensile strength 4.5 kN) was considered (Section 2.3). Referring to a longitudinal, reinforced masonry wall portion 4000 mm wide, according to the procedure described in Section 2.3, the initial stiffness was evaluated equal to 2.68 kN/mm ($3E_{cr}I/L^3$) while the first cracking load, $F_{cr(R)}$ = 13.0 kN, the ultimate resistance $F_{u(R)}$ = 19.4 kN and the ultimate displacement $s_{u(R)}$ 196 mm. The collapse of transversal, reinforced masonry walls resulted governed by in-plane bending failure (global wall resistance V_{Rd} (M_0) = 257.6 kN, V_{Rd} (M_u) = 526.9 kN). It is observed that a halved Young modulus was assumed for the reinforced masonry (cracked masonry). The analysis results showed a global collapse governed by the bending failure of the transversal walls, attained for a horizontal displacement of the control point equal to 8.7 mm (Fig. 7a). The equivalent springs of the roof attained to a maximum axial load of 103.5 kN (Fig. 6c) and the resistant ground acceleration $a_{g,res}$ was equal to 0.330 g.
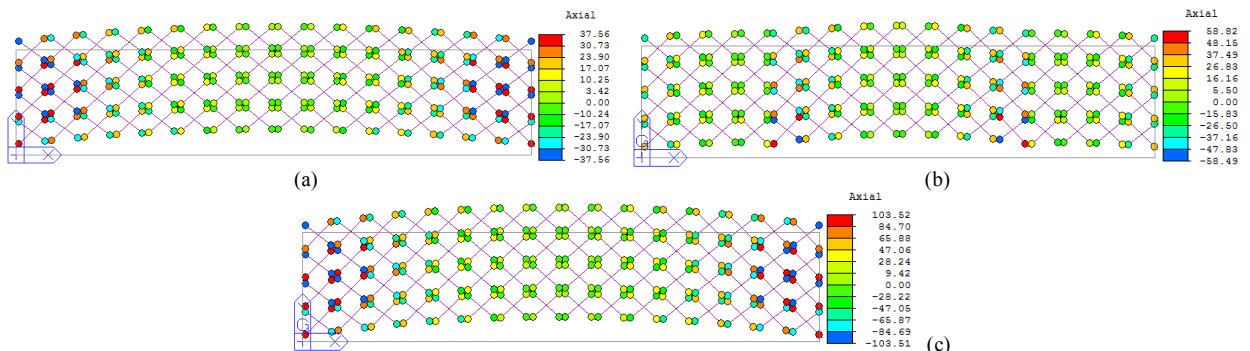

Fig. 6. Axial load in diagonal springs representing the roof bracing, when the global ultimate displacement of the structure is attained: (a) Case B, (b) Case C and (c) Case D

In Fig. 7a, a comparison among the capacity curves of the three analyzed configuration is illustrated. In Fig. 7b the resistant ground accelerations are compared: it is observed that in "Case B" a value slightly higher than "Case A" was attained (1.1 times), while in cases "C" and "D", $a_{g,res}$ was equal to 1.9 e 2.7 times that of "Case A", respectively.
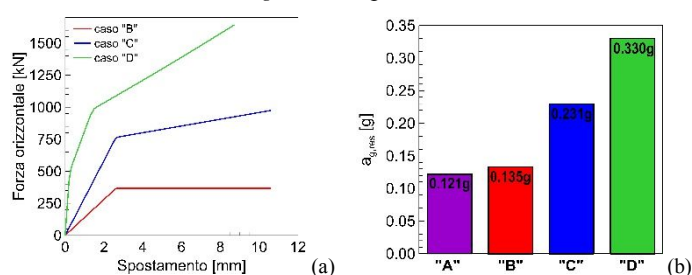

Fig. 7. Comparisons of the different analysed configurations in terms of (a) capacity curves and (b) resisting ground acceleration

5. Conclusions

Strategies for the reduction of the seismic vulnerability of historical industrial buildings with traditional multi-slope timber roofs, laid on masonry walls along the perimeter and internally on point supports, are investigated in the paper. A simplified numerical method was presented to analyze the effects of a roof bracing by means of nailed wooden-based panels ("Case B"), also integrated with the introduction of steel portal frames ("Case C") or with the strengthening of the perimeter walls by means of a mortar coating with composite meshes embedded ("Case D"). For the evaluation of the behavior of the different resisting elements, analytical correlations were proposed.

A representative case study was analyzed: with respect to the actual situation ("Case A"), it was observed that the increase in resistant ground acceleration due to the roof bracing only (Case "B") is very limited (12%), due to the premature collapse of the transversal walls. It is therefore necessary to associate this intervention for example with the introduction of steel metal portal frames (Case "C") or with the reinforcement of the walls. Considerable resistant ground accelerations were attained in these cases (0.23 - 0.31 g, respectively).

Acknowledgements

References

CSLP - Consiglio Superiore dei Lavori Pubblici. (2009). Circolare 2 febbraio 2009, n. 617. Istruzioni per l'applicazione delle "Nuove norme tecniche per le costruzioni" di cui al decreto ministeriale 14 gennaio 2008, Italy.

FEMA 273. (1997). NEHRP guidelines for the seismic rehabilitation of buildings. Washington, D.C.

Gattesco. N., Boem, I. (2015a). Seismic performances and behavior factor of post-and-beam timber buildings braced with nailed shear walls, *Engineering Structures*, 100, 674–685.

Gattesco. N., Boem, I. (2015b). Experimental and analytical study to evaluate the effectiveness of an in-plane reinforcement for masonry walls using GFRP meshes. *Construction and Building Materials*, 88, 94-104.

Gattesco. N., Boem, I. (2016). Stress distribution among sheathing-to-frame nails of timber shear walls related to different base connections: Experimental tests and numerical modelling. *Construction and Building Materials*, 122, 149-162.

Gattesco. N., Boem, I. (2017a). Out-of-plane behavior of reinforced masonry walls: experimental and numerical study. *Composites Part B: Engineering*, 128, 39-52.

Gattesco, N., Boem, I. (2017b). Characterization tests of GFRM coating as a strengthening technique for masonry buildings. *Composite Structures*, 165, 209-222.

Gattesco, N., Boem, I. (2017c). Assessment of the seismic capacity increase of masonry buildings strengthened through the application of GFRM coatings on the walls. *Int. J. Masonry Research and Innovation*, 2(4), 300-320.

Magenes, G., Calvi, G.M. (1997). In-plane seismic response of brick masonry walls. Earthquake Eng. and Structural Dynamics, 26, 1091–1112.

Sisti, R., Corradi, M., Borri, A. (2016). An experimental study on the influence of composite materials used to reinforce masonry ring beams. *Construction and Building Materials*, 122, 231–241.

Turnsek, V., Cacovic, A. (1971). Some experimental results on the strength of brick masonry walls. 2nd International Brick Masonry Conference, 12-15 April, Stoke on Trent, United Kingdom.